Supporting information

Optical Tracking of Nanometer-Scale Cellular Membrane Deformation Associated with Single Vesicle Release

Fenni Zhang*[1,3], Yan Guan*[1,3], Yunze Yang[1,3], Ashley Hunt[1], Shaopeng Wang[1], Hong-Yuan Chen[2], and Nongjian Tao**[1,3]

1. Biodesign Center for Bioelectronics and Biosensors, Arizona State University, Tempe, AZ 85287, USA.

2. State Key Laboratory of Analytical Chemistry for Life Science, School of Chemistry and Chemical Engineering, Nanjing University, Nanjing 210093, China

3. School of Electrical Computer and Energy Engineering, Arizona State University, Tempe, Arizona 85287, USA.

*These authors contribute equally to the project.

**Corresponding authors. njtaob@gmail.com

Abstract

Exocytosis involves interactions between secretory vesicles and the plasma membrane. Studying the membrane response is thus critical to understand this important cellular process and to differentiate different mediator release patterns. Here we introduce a label-free optical imaging method to detect the vesicle–membrane-interaction-induced membrane deformation associated with single exocytosis in mast cells. We show that the plasma membrane expands by a few tens of nanometers accompanying each vesicle-release event, but the dynamics of the membrane deformation varies from cell to cell, which reflect different exocytosis processes. Combining the temporal and spatial information allows us to resolve complex vesicle-release processes, such as two vesicle-release events that occur closely in time and location. Simultaneous following a vesicle release with fluorescence and membrane deformation tracking further allows us to determine the propagation speed of the vesicle-release-induced membrane deformation along the cell surface, which has an average value of 5.2 ± 1.8 μm/s.

S-1. Calibration of differential optical tracking of cell membrane deformation

The differential optical tracking method provides precise measurement of cell membrane deformation, but it requires calibration to relate the differential imaging intensity (see main text) to an actual deformation in nm. This was performed with the following procedures: (1) The edge of cell and its centroid were determined with an imaging-processing algorithm. (2) A rectangular region of interest (ROI) was selected at a location along the cell edge such that the cell edge passes through the center of the ROI in a direction parallel to one side of the rectangle (Fig. S1-A). The ROI is then divided in two regions along the center (blue and red boxes) with image intensities denoted as I_1 and I_2, respectively. (3) At each location, calibration is performed by shifting the ROI by a certain number of pixels from inside to outside of the cell (Fig. S1-B). The corresponding differential image intensity, I_1-I_2/(I_1+I_2), was determined vs. the number of pixel shift, which displays a linear regime (between two dashed lines in Fig. S1-C). (4) The pixel numbers were converted into nm by considering the pixel size and magnification factor of the optical microscope, which leads to a calibration curve (Fig. 1S-D). (5) The same calibration procedure is repeated at each location along the cell edge by rotating the ROI around the centroid every degree per location.

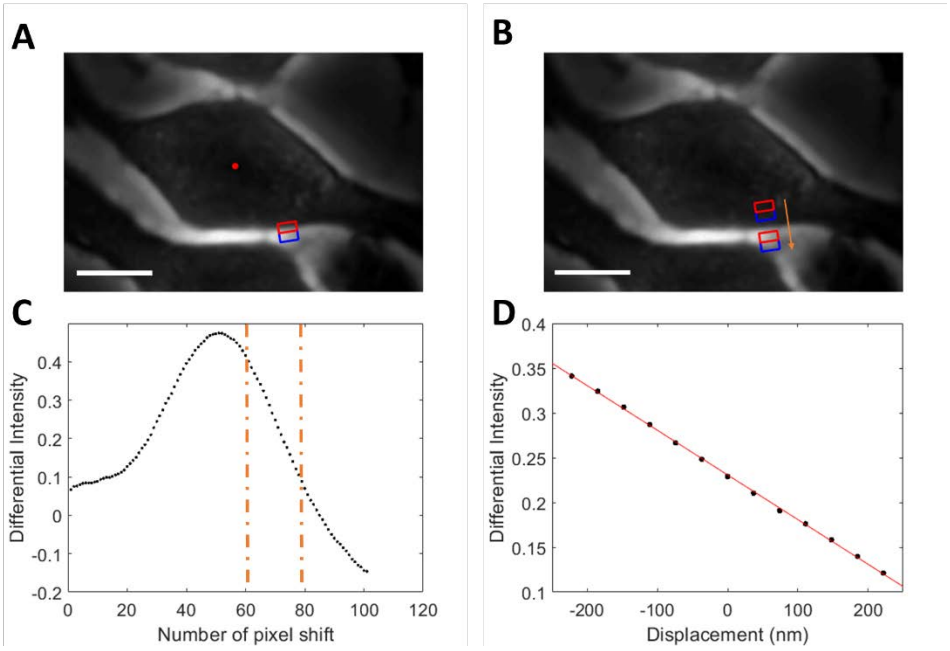

Fig. S1 Calibration of the optical tracking of cellular deformation. (A) A rectangular region of interest (ROI) (1.11 μm x 2.22 μm) is selected to include the edge of a cell for differential image intensity calculation and the centroid of the cell is identified (red dot). (B) The ROI is shifted by different numbers of pixels from inside to outside of the cell in the direction perpendicular to the tangential line at the cell edge and the corresponding differential image intensity is determined. (C) Differential image intensity vs. ROI shifting in terms of pixel numbers, which shows a linear regime marked by two vertical dotted lines. (D) From the pixel size and optical magnification of the optical microscope, the pixel numbers in C are converted to the actual displacement of the ROI in terms of nm, which provides a calibration curve. The same procedure is repeated for each point along the cell edge. Scale bar: 10 μm.

S-2. Optical synchronization

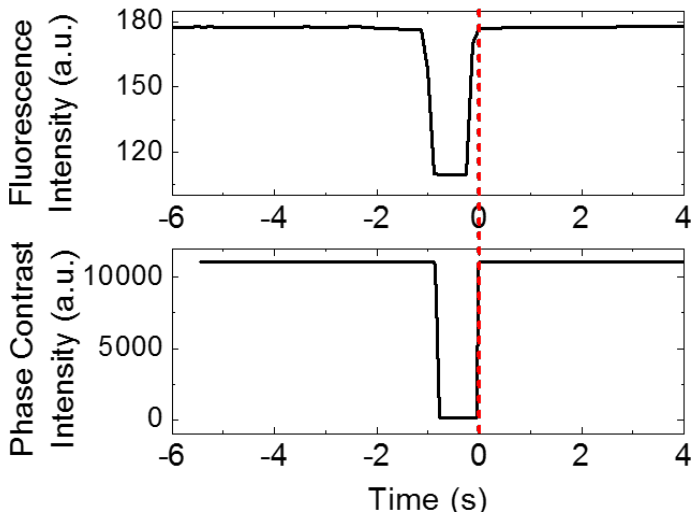

Fig. S2 Synchronization of phase contrast and fluorescence image recording. A shutter is used to block the common light path of fluorescence and phase contrast imaging, which creates well defined drops in both the fluorescent and phase contrast image intensities. Aligning the edge of the intensity drops allows synchronization of the simultaneously recorded fluorescent and phase contrast images.

S-3. Cell membrane deformation at different locations

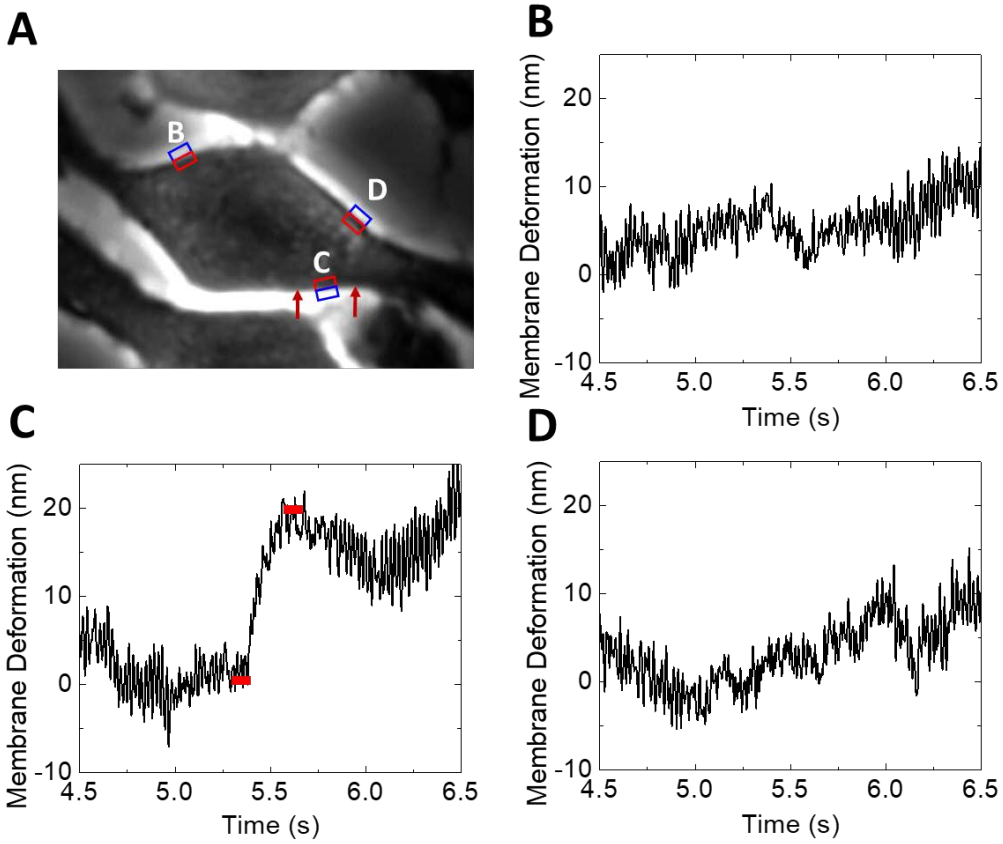

Fig. S3 Membrane Deformation at different locations along a cell edge. (A) Phase contrast image of a RBL-2H3 cell, where ROIs at three locations are labeled by B, C, and D. (B-D) Membrane deformation at the locations marked by B, C and D, respectively.

S-4. Membrane deformation histogram of individual granule release events in different cells

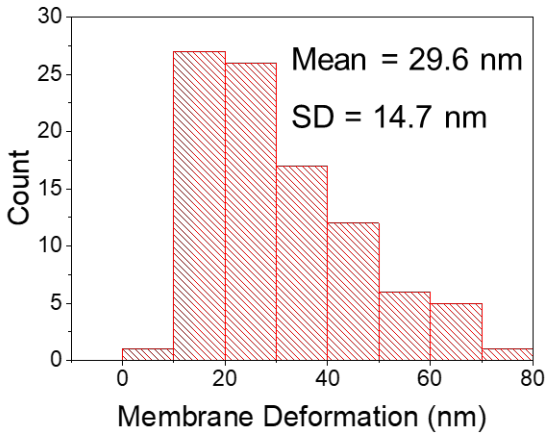

Fig. S4 Distribution of maximum membrane deformations induced by individual granule release events (n=95) in different cells.

S-5. Examples of different patterns of granule release-induced membrane deformation

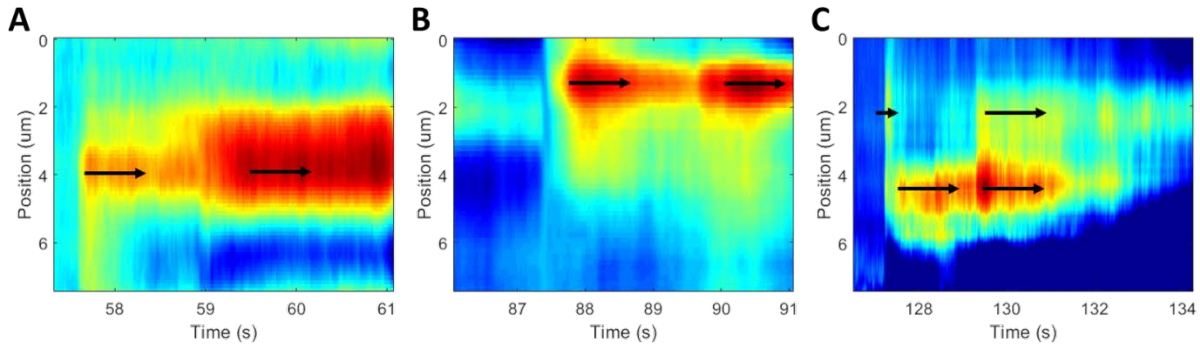

Fig. S5 Temporal-spatial correlation mapping showing (A) Two consecutive granule release events at the same location (a small one followed by a large one). (B) Two consecutive granule release events at the same location with similar amount of membrane deformation. (C) Four granule release events.